

# **WIND ENERGY HARVESTING USING SRG**

*Thesis submitted by*

**Mithool Jain and Soham Roy**

*under the guidance of*

**Prof. G. Bhuvaneswari**

*in partial fulfilment of the requirements  
for the award of the degree of*

**Bachelor of Technology**



**Department of Electrical Engineering  
INDIAN INSTITUTE OF TECHNOLOGY DELHI**

**November 2017**

## THESIS CERTIFICATE

This is to certify that the thesis titled **Wind Energy Harvesting Using SRG**, submitted by **Mithool Jain and Soham Roy**, to the Indian Institute of Technology, Delhi, for the award of the degree of **Bachelor of Technology**, is a bona fide record of the research work done by them under my supervision. The contents of this thesis, in full or in parts, have not been submitted to any other Institute or University for the award of any degree or diploma.

**Prof. G. Bhuvaneswari**  
Professor  
Dept. of Electrical Engineering  
IIT-Delhi

Place: New Delhi

Date: 17th November 2017

## **ACKNOWLEDGEMENTS**

Thanks to Prof. G. Bhuvaneswari for her immense guidance, support, and motivation throughout this project.

# **ABSTRACT**

**KEYWORDS:** wind energy conversion; switched reluctance machine; generation

There has been significant breakthrough in the fields of power semiconductor devices and renewable energy over the recent years. With the advent of renewable sources like wind energy and solar power, there is a need for active research in these fields which will serve as the primary sources of energy in the future. Wind energy harvesting has seen tremendous popularity in the western world since the 1980s and has been recently gaining popularity in India too. A lot of research and developmental activities have been carried out on variable speed and fixed speed systems for wind energy conversion.

The Switched Reluctance Machine (SRM) is a robust and versatile machine suitable for high speed operation as motor and its functioning as a motor has been investigated extensively. However, its generation operation is relatively unexplored. A remarkable property of this machine is that its torque production can be controlled simply by controlling the interval of angles (dwell angle) for which a rotor phase is excited. This paper is an attempt to explore the operation of an SRM as a Switched Reluctance Generator (SRG) coupled to a wind-turbine as a part of a wind energy conversion system (WECS). An effort has been made to obtain a tangible output power by adjusting the turn on and turn off angles, on and off respectively, for the associated converter for each of the phases. The converter configuration used is like a two-quadrant chopper which is known as asymmetric converter. The entire system has been modelled and simulated in Simulink/MATLAB environment and the results obtained under different operating conditions have been presented to show the effectiveness of the control configuration.

# Contents

<b>ACKNOWLEDGEMENTS</b>	<b>i</b>
<b>ABSTRACT</b>	<b>ii</b>
<b>LIST OF TABLES</b>	<b>iv</b>
<b>LIST OF FIGURES</b>	<b>v</b>
<b>ABBREVIATIONS</b>	<b>vi</b>
<b>NOTATION</b>	<b>vii</b>
<b>1 INTRODUCTION</b>	<b>1</b>
1.1 General. . . . .	1
1.2 Motivation and Background. . . . .	1
1.3 Scope of Work. . . . .	3
1.4 Organisation of the report. . . . .	3
<b>2 SYSTEM CONFIGURATION</b>	<b>4</b>
2.1 Converter. . . . .	4
<b>3 SIMULATION AND MODELLING OF 6/4 SRM</b>	<b>5</b>
3.1 Inductance profile. . . . .	5
3.2 Running as a Motor . . . . .	6
3.3 Regenerative Operation . . . . .	7
3.4 Operation as Generator. . . . .	8
<b>4 SIMULATION AND MODELLING OF 8/6 SRM</b>	<b>10</b>
4.1 Choice of Converter . . . . .	10
4.2 Magnetisation Character. . . . .	10
4.3 Inductance profile. . . . .	11
4.4 Using capacitor for excitation. . . . .	12
4.5 Using Buck Converter at load end. . . . .	12
<b>5 MAXIMUM POWER POINT TRACKING USING 8/6 SRG</b>	<b>14</b>
5.1 Tracking reference rotor speed using turbine characteristics. . . . .	14
5.2 Performance in dynamic wind speed conditions. . . . .	14
<b>6 CONCLUSIONS</b>	<b>16</b>
6.1 Objectives met. . . . .	16
6.2 Steps involved. . . . .	16
6.3 Conclusion. . . . .	16
<b>APPENDIX</b>	<b>17</b>
<b>Bibliography</b>	<b>18</b>
<b>LIST OF PAPERS BASED ON THESIS</b>	<b>19</b>

# List of Tables

3.4.1	Results of energy harvested using 6/4 pre-set model. . . . .	9
5.2.1	Power supplied and converted with MPPT. . . . .	14

## List of Figures

1.1.1	6/4 SRM in aligned position (left) and unaligned position (right) . . . . .	2
2.1	System configuration. . . . .	4
2.1.1	Asymmetric converter for SRM . . . . .	4
3.1.1	Inductance profile of SRM: Rising region (left) and Falling region (right)	5
3.1.2	Current chopping mode (left) and Single pulse mode (right) . . . . .	6
3.2.1	Comparison of actual and calculated torques . . . . .	6
3.3.1	Simulink model used for regenerative braking. . . . .	7
3.3.2	Torque and speed waveforms for motoring operation followed by regenerating (left); current waveforms for regenerative operation (right) . . . .	8
3.4.1	Simulink model for generation using 6/4 SRM. . . . .	8
3.4.2	Waveforms of generated torque, machine speed and supplied mechanical power (left); current and electrical power generated (right) . . . . .	9
4.2.1	Magnetisation characteristics of 4 kW, 4-phase, 8/6 pole Oulton, TASC, SRM . . . . .	10
4.3.1	Calculated inductance profile for of 4 kW, 4-phase, 8/6 pole Oulton, TASC, SRM. . . . .	11
4.4.1	Simulink model for generation using 8/6 SRM. . . . .	12
4.4.2	Infinite charging of capacitor in absence of dissipative element. . . . .	12
4.5.1	Buck Configuration to keep constant capacitor voltage. . . . .	13
4.5.2	Waveforms for Buck Converter operation maintain constant capacitor voltage. . . . .	13
5.2.1	Simulation result for tracking maximum power point with changing wind speed. . . . .	15
5.2.2	Turbine characteristic showing maximum power point at 9.6 m/s (left) and 12 m/s (right) . . . . .	15

## **ABBREVIATIONS**

<b>PM</b>	Permanent Magnet
<b>SRM</b>	Switched Reluctance Machine/Switched Reluctance Motor
<b>SRG</b>	Switched Reluctance Generator
<b>FTBL</b>	Flux lookup table
<b>ITBL</b>	Current lookup table
<b>TTBL</b>	Torque lookup table
<b>WECS</b>	Wind Energy Conversion System
<b>MPP</b>	Maximum Power Point
<b>MPPT</b>	Maximum Power Point Tracking



## NOTATION

$\lambda$	Flux linkage/Tip Speed Ratio
$\theta$	Rotor angle
$I, i$	Stator Current
$\beta$	Turbine Blade Pitch Angle
$\theta_{on}$	Phase Turn On Angle
$\theta_{off}$	Phase Turn Off Angle
$\omega_{ref}$	Reference Speed of Machine
$L$	Stator Winding Inductance
$J$	Machine Moment of Inertia
$T_e$	Electromagnetic Torque
$T_m$	Load/Mechanical Torque

---

# Chapter 1

## INTRODUCTION

### 1.1 General

Switched reluctance machines (SRMs) possess a doubly-salient structure with passive rotors. They are quite popular in applications that require variable speed operation. Owing to the absence of permanent magnets (PMs) or rotor windings, their rotors have a lower inertia. Moreover, they are less costly, easy to manufacture, and can operate at high speeds as well as high temperature. Most of the losses of the machine are eliminated due to the absence of windings on the rotor, typically present in other machines. SRMs are often employed as motors in numerous applications like high speed centrifuges, water pumping and electric vehicles [1-3]. It is necessary to have accurate rotor position information for the SRM to run successfully. The effectiveness of the SRM as a maintenance-free motor drive is compromised due to the presence of rotor position sensor. Torque ripples are one of the most significant problems faced in the application of SRM in any of the noise-free applications. Several works in literature in the past have addressed minimisation of the torque ripple of SRMs by various intelligent control strategies [4-6], out of which some are sensor-less techniques as well.

### 1.2 Motivation and Background

Traditionally for megawatt-range wind energy harvesting applications, the induction machine is used. Permanent magnet generator is another suitable but costly alternative, due to the magnetic material cost. On the contrary, such designs reduce the requirement of maintenance associated with rotating contacts as they result in improved efficiency and remove the necessity of using starting capacitor banks [12].

Although SRM drives have been researched extensively, still this machine working as a generator has not been investigated thoroughly. One of the papers investigate this machine functioning as a generator during braking operation [7]. Small scale wind energy system applications advocate SRM as a viable option due to its maintenance-free operation. Switched Reluctance Generators (SRGs) are also being put forth as a generator suitable for automotive applications [8-10].

SRM contains saliency in both its stator and rotor (Figure 1.1.1). As any point of time, only one stator phase is excited. As a result, the varying positions of the rotor with respect to the stator during its rotation lead due varying values of reluctance for the established flux linkage. In the aligned position, the rotor and stator phases are in phase – thus giving a minimum reluctance path. On the other hand, the unaligned position leads to maximum reluctance or minimum inductance.

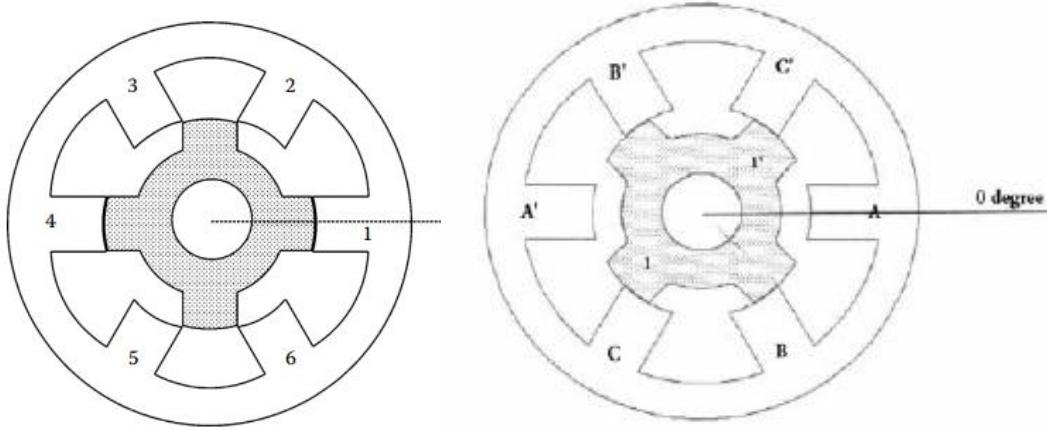


Figure 1.1.1: 6/4 SRM in aligned position (left) and unaligned position (right)

We can write the basic KVL equation to describe the working of the Switched Reluctance machine:

$$V = RI + \frac{L(\theta)dI}{dt} + \frac{I(\omega)dL}{d\theta} \quad (1.2.1)$$

Here the last term corresponds to the back EMF,  $E_b = \frac{I\omega dL}{d\theta}$ , like a DC machine. Consequently, by applying the power balance condition at equilibrium, the torque delivered by the machine is obtained as:

$$T_e = \frac{1}{2}i^2 \left( \frac{dL}{d\theta} \right) \quad (1.2.2)$$

Through this expression, one can see that the sign of current  $i$  is immaterial sign of torque delivered; hence its sign is governed by that of  $\frac{dL}{d\theta}$  alone. Since SRM is a reluctance machine, its tendency is to always try to reach the maximum inductance position so that it can minimise reluctance to the flux linkage (thereby minimising the stored energy). In motoring operation, it is known that positive torques must be produced, so  $\frac{dL}{d\theta}$  must be positive. Therefore, the chosen values of  $\theta_{on}$  and  $\theta_{off}$  must lie in the rising inductance region. Whereas for generation, negative torques must be produced, and  $\theta_{on}$  and  $\theta_{off}$  must be chosen in the falling inductance region.

---

## 1.3 Scope of Work

This project is an attempt towards choice of suitable switching angles for obtaining a substantial amount of power in generation mode from a switched reluctance machine using an asymmetric converter. This generator can be used in Wind Energy Conversion Systems (WECS) to harvest wind energy and maximum power point (MPP) can be continuously tracked to enable harvesting optimal amount of energy.

## 1.4 Organisation of the report

This chapter introduced the operation of SRM. The rest of the report is organised as follows: Chapter 2 describes the Literature Review followed by Chapter 3 which presents the System Configuration. Chapter 4 describes the modelling and simulation of 6/4 SRM in motoring, regenerative and generation modes of operation. Chapter 5 describes the modelling and simulation of 8/6 SRG. Chapter 6 describes maximum power point tracking and the results obtained. Chapter 7 presents the conclusions.

## Chapter 2

### SYSTEM CONFIGURATION

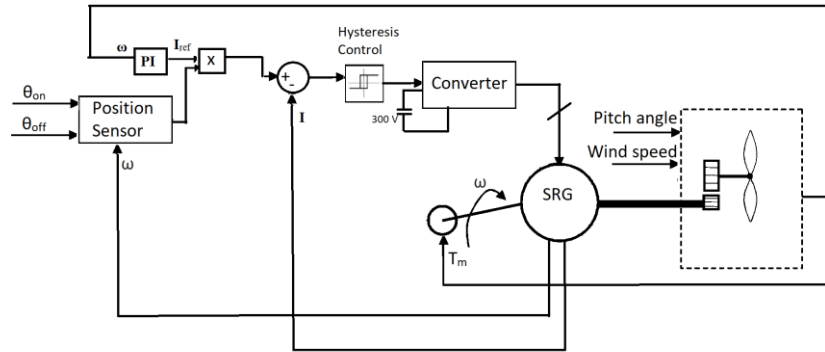


Figure 2.1: System configuration

The system comprises a wind turbine which drives an SRG through a gear box of ratio 0.8: 1 (Figure 2.1). A converter is connected to the output phases of the SRG and the power generated is fed to a common DC bus. The control of the converter is performed by measuring the terminal voltages and currents of the machine.

### 2.1 Converter

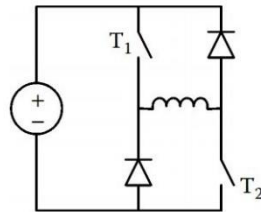


Figure 2.1.1: Asymmetric converter for SRM

In this work, asymmetric converter has been used whose circuit diagram for one phase is shown in Figure 2.1.1. The devices  $T_1$  and  $T_2$  could be IGBTs or any of the self-commutating devices whereas the diodes are the ones which are instrumental in circulating the generated power.  $T_1$  and  $T_2$  are used for exciting the phase winding. The overall power fed back by the diodes should be more than the power taken by the phase winding for excitation. Only under this condition, the machine will be functioning in generating mode.

The subsequent two chapters will look at the modelling of simulations of 6/4 SRM and 8/6 SRM in various modes, with emphasis on generation.

## Chapter 3

### SIMULATION AND MODELLING OF 6/4 SRM

The initial work was carried out using a pre-set model of a 6/4 Switched Reluctance Machine of 60 kW rating available in Simulink. This model was thoroughly tested by simulating its operation in both motoring and generating regions. To optimise the switching angles, the machine was first simulated in the motoring mode using the same asymmetric converter and then, the switching angles were shifted so that the machine goes into generating region. The parameters of the machine under consideration are given in Appendix A.1

#### 3.1 Inductance profile

The model has a pre-fed flux lookup table (FTBL) which contains the data points for the  $\lambda$ -i- $\theta$  characteristics of the machine. Simulink uses this table to calculate the corresponding currents and torques to obtain the current lookup table (ITBL) and torque lookup table (TTBL) respectively. We used asymmetric converter (Figure 2.1.1) for exciting the different phases of the machine using battery as an excitation source. When the switches T1 and T2 are on, the current flows through the IGBTs to excite one phase of the machine, thereby increasing its magnetic field energy. The switches in the off state, on the other hand, allow current to flow through the diodes back into the battery which allows de-fluxing, or regenerative action. This is what allows the machine phase winding to return its energy.

Initially the inductance profile of the machine has been plotted using  $L = \frac{\lambda}{i}$  for both high speed and low speed operation (Figure. 3.1.1). This allowed us to suitably identify the appropriate ranges of  $\theta_{on}$  and  $\theta_{off}$  for the motoring and generating operations. As can be seen in the figure, it was found that the inductance profiles were almost identical for high and low speeds. The machine can be usually run in two different modes according to the speed at which it is running [11]: (a) current chopping mode, and (b) single pulse mode, for low and high speeds of operation respectively.

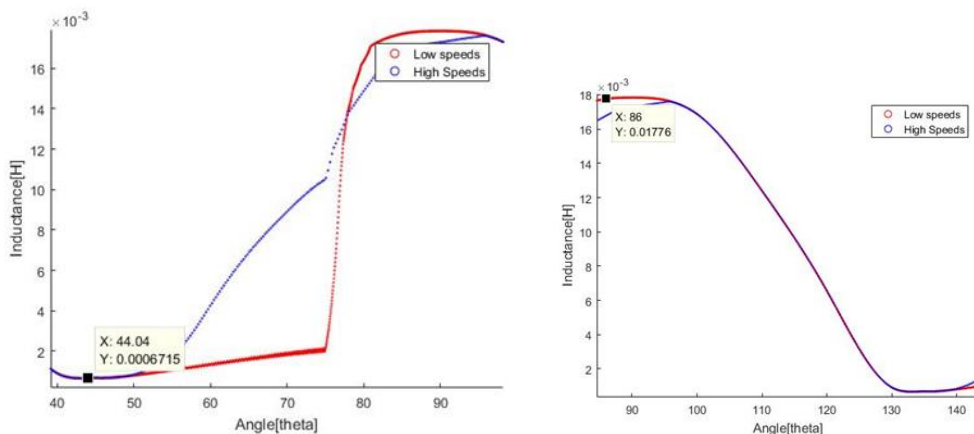


Figure 3.1.1: Inductance profile of SRM: Rising region (left) and Falling region (right)

When the machine is running at low speeds, the current gets a long time to rise. It might as well reach a dangerously high value, if not controlled properly. To control the current, we employ current chopping (or regulation) by using a hysteresis current controller. Contrarily, during high speed operation of the motor, there is limited time for the current to rise. It is observed the current encounters a single peak for the motoring operation, while the IGBT switches are on. Subsequently, the current is found to die down to zero during the interval when the diodes are conducting (Figure 3.1.2).

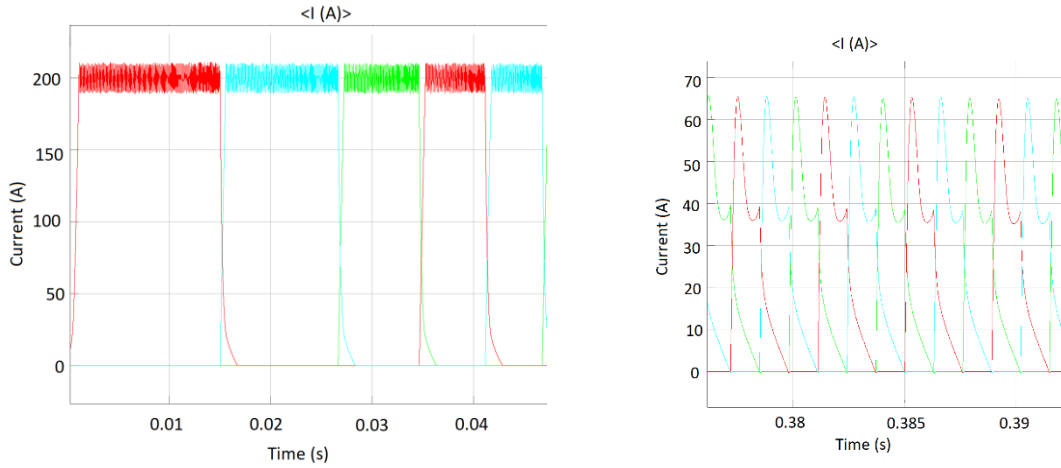


Figure. 3.1.2: Current chopping mode (left) and Single pulse mode (right)

## 3.2 Running as a motor

First, the machine was operated in motoring mode, with the default turn on and turn off angles  $\theta_{on} = 45^\circ$  and  $\theta_{off} = 75^\circ$  respectively. For each phase, torques obtained from (2) were computed and then compared against the torque values obtained from the  $T_e$ - $i$ - $\theta$  lookup table in the machine model. The profile of the total torque was found to be almost like that obtained from the look-up table (Figure 3.2.1). The positive torques obtained from the machine confirmed that it was operating in the motoring region.

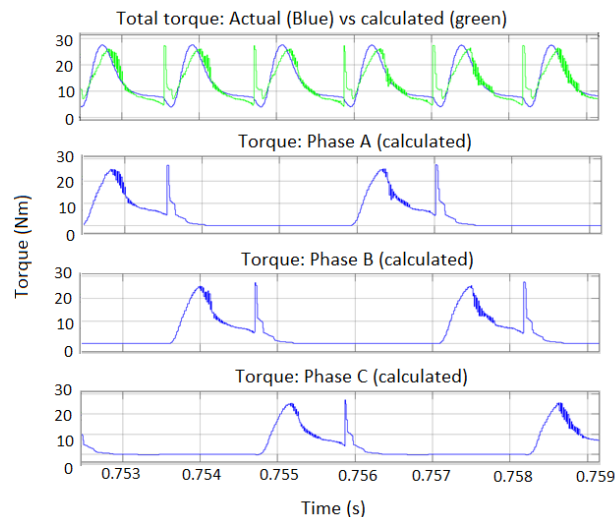


Figure. 3.2.1: Comparison of actual and calculated torques

### 3.3 Regenerative Operation

The machine was then operated in regenerative mode (Figure 3.3.1), before exploring its standalone generation. The falling inductance profile (Figure 3.1.1) was used for choosing appropriate values of  $\theta_{on}$  and  $\theta_{off}$  for the regenerative mode. For operation at rated speed, various values of  $\theta_{on}$  were tried and tested. Based on the observations of torque,  $85^\circ$  was found to be the optimal value of  $\theta_{on}$ , around which the inductance is constant. This permits the current to get enough time to rise to a sufficient value before encountering the falling inductance region. Furthermore,  $\theta_{off}$  was also chosen in a similar fashion. It was found to be optimal around  $110^\circ$ , which allows the currents to die down before the next rise in the inductance profile (this avoids the generation of motoring torque). These values of  $\theta_{on}$  and  $\theta_{off}$  were found to yield the maximum average negative torque. These values of  $\theta_{on}$  and  $\theta_{off}$  would also allow the machine to run in regenerative operation at low speeds. However, the optimal  $\theta_{on}$  values for low speed were higher, which would mean that the phase would be excited just slightly in advance with respect to the falling inductance region. This is because the current has sufficient time to rise to an appreciable value in a small time at lower speeds.

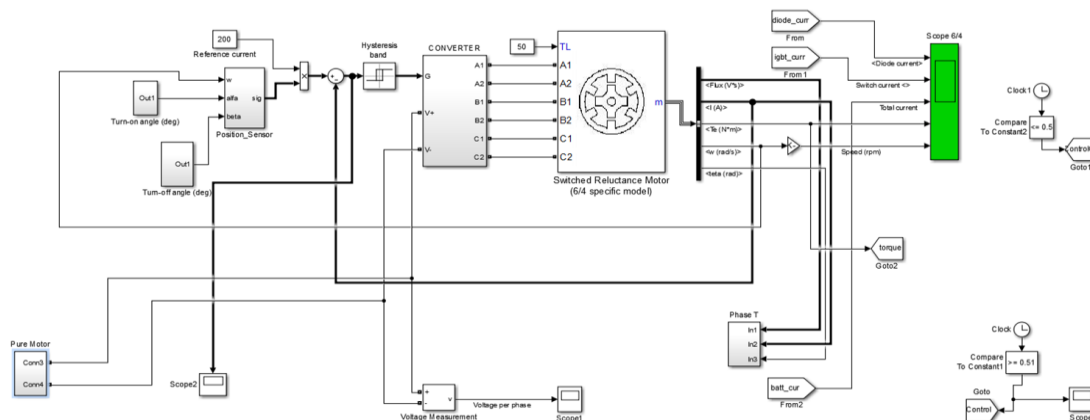


Figure 3.3.1: Simulink model used for regenerative braking

The machine was first started as a motor and allowed to attain steady state, with its  $\theta_{on}$  and  $\theta_{off}$  corresponding to that for the motoring region (Figure 3.3.2). Upon attaining its steady state speed and constant torque, it was switched to regenerative mode by changing  $\theta_{on}$  and  $\theta_{off}$  to  $85^\circ$  and  $110^\circ$  respectively. Here, the motor feeds back power to the supply and the torque is produced in a sense that it opposes the speed of the machine.

Regeneration was tried out in three different approaches: first, a load resistance was used to replace the battery like in the case of dynamic braking in DC machines. But the flux was found to disappear within a fraction of a second. The second approach was to use an excitation capacitance with shunt load to sustain the flux. This led to some negative torques, but the flux still died out. Finally, regeneration was carried out with a battery itself. This approach was found to yield a decrease in speed, as observed in the usual case of braking in DC machines. This was due to the



production of negative torques and the energy being fed back into the battery (Figure 3.3.2).

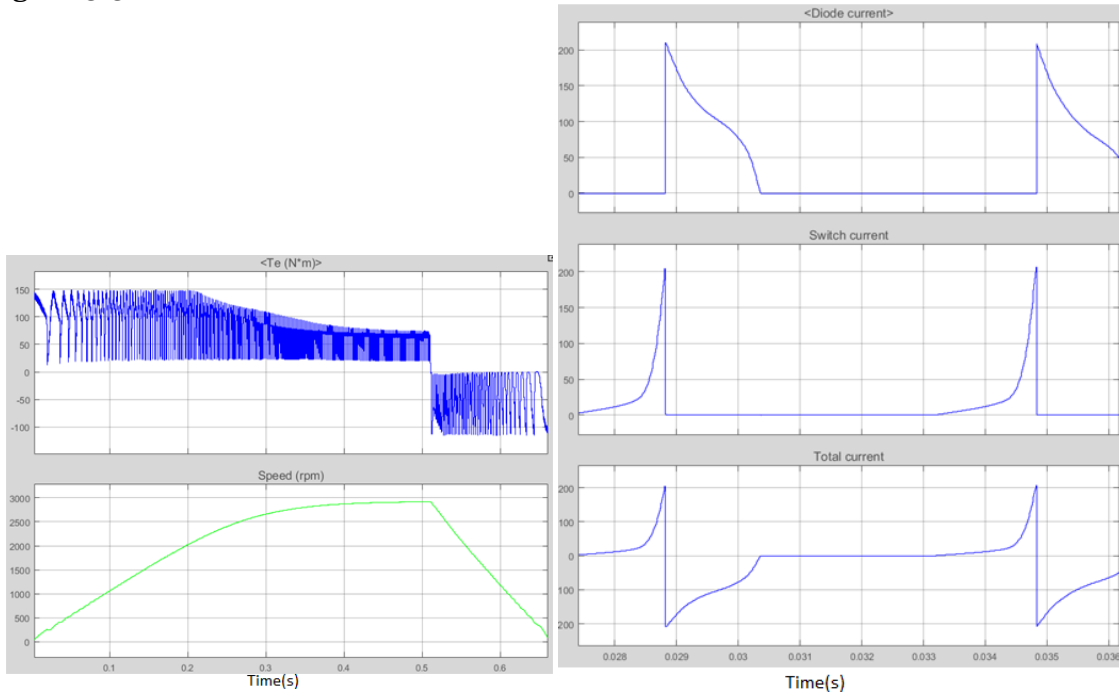


Figure 3.3.2: Torque and speed waveforms for motoring operation followed by regenerative (left); current waveforms for regenerative operation (right)

### 3.4 Operation as generator

After successful regenerative braking operation in motor, the model was extended to run the machine as a generator coupled to a wind turbine (Figure 3.4.1). The load for the generator was taken as a battery into which generated energy could be fed. For the generation mode, negative torque is needed, for which the values of turn-on ( $\theta_{on}$ ) and turn-off ( $\theta_{off}$ ) angles were selected as  $\theta_{on} = 85^\circ$  and  $\theta_{off} = 110^\circ$  like the regenerative mode.

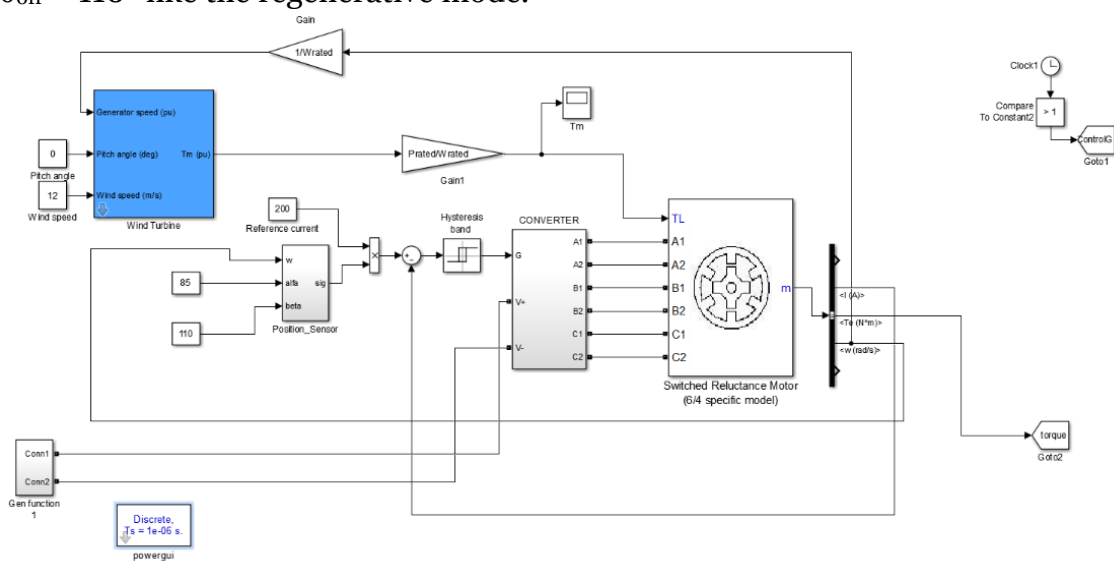


Figure 3.4.1: Simulink model for generation using 6/4 SRM

The base speed of the wind turbine was chosen as 0.667 times that of the

generator base speed. This was done to keep the no load speed of the machine within its rated speed. The generator was kept in unloaded condition for the initial 0.1s. The mechanical torque provided by the wind turbine during this time helped the machine reach its rated speed of 3000 rpm.

Then the circuit breaker contacts were closed, thus connecting the battery across the generator terminals which served as the load to the SRG. The average current entering the battery was found to be positive, thus establishing that the energy is fed to the battery from the machine, thus charging the battery. The torque produced is also observed to be negative while it is rotating with a positive  $\omega$  value, which is a typical characteristic of a generation operation.

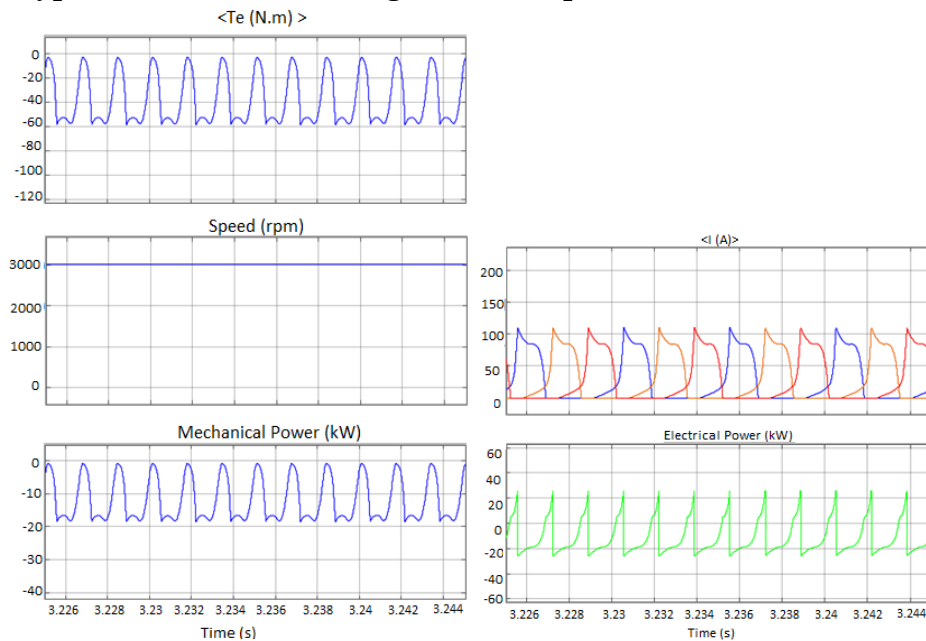


Figure 3.4.2: Waveforms of generated torque, machine speed and supplied mechanical power (left); current and electrical power generated (right)

The waveforms for torque, speed, mechanical power, current and electrical power have been shown at steady state (Figure 3.4.2). The speed was constant, owing to steady state operation. Instantaneous torque was found to oscillate between -2 Nm and -58 Nm, with an average value of -38 Nm. The mechanical power delivered was also seen to oscillate between -2 kW and -16 kW, with an average value of -11.93 kW. The current in each phase was observed to have a peak, followed by a gradual decrease in the region where IGBTs conduct. The results obtained are tabulated in Table 3.4.1.

Table 3.4.1: Results of energy harvested using 6/4 pre-set model

Electrical Power received by battery, $P_e$	11.44 kW
Mechanical Power supplied $P_m$	-11.93 kW
Average Torque, $T_e$	-38.14 N.m

This chapter looked into the motoring, regeneration and generation modes of operation of 6/4 SRM. The next chapter will deal with the generation mode of 8/6 SRM.

## Chapter 4

### MODELLING AND SIMULATION OF 8/6 SRM

Subsequent simulations were carried out using an 8/6 switched reluctance machine of 4 kW like the one available in the lab (Appendix A.2). This is a more realistic machine than the one that was being used previously.

#### 4.1 Choice of converter

Since there are even number of pole pairs in the rotor, it is possible to use a midpoint converter instead of an asymmetric converter that was used for the 6/4 case. However, there is no significant mention in literature regarding the usage of a midpoint converter in generation operation. Therefore, the generation operation in this case was also carried out using an asymmetric converter.

#### 4.2 Magnetisation characteristic

The method of determining saturation characteristics, described in [13] was carefully studied. In this method, a phase is excited for a very short interval of time and a dc voltage is applied. The he current and voltage transients are measured during the interval in which the phase is excited. Consequently, the flux linkage is obtained using  $d\psi = \{v(t) - Ri(t)\}dt$ . This entire procedure was repeated for different positions of the rotor w.r.t. stator.

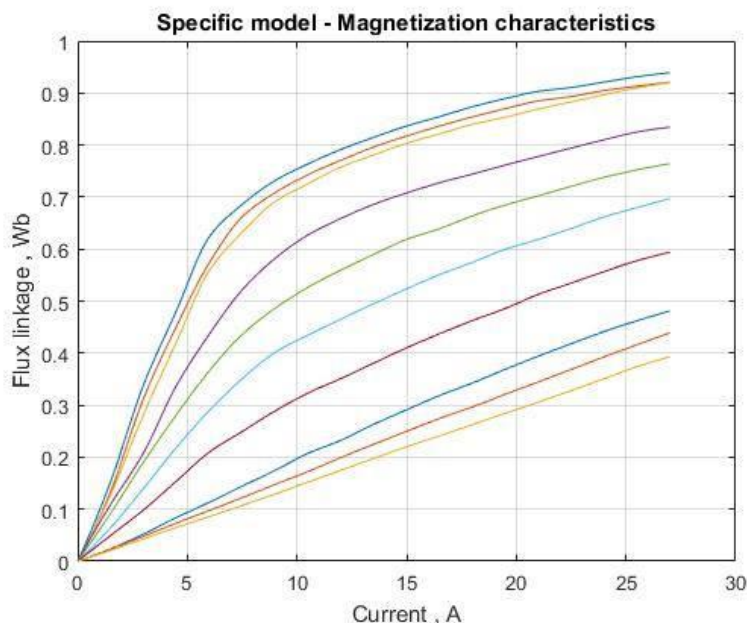


Figure 4.2.1. Magnetisation characteristics of 4 kW, 4-phase, 8/6 pole Oulton, TASC, SRM

Due to logistics constraints, the magnetisation characteristic was obtained from

the paper, to simulate a machine which would be realistic enough. The value of rotor angle  $\theta$  was varied from  $0^\circ$  to  $30^\circ$  in steps of  $2^\circ$ , and the stator current  $i$  was varied from 0 to 29 A – the flux linkage for each of these points was obtained. This magnetisation characteristic was fed as the FTBL of the new machine and the plot generated by Simulink is shown in Figure 4.2.1.

### 4.3 Inductance profile

As before, the inductance was obtained for various values of  $\theta$  using the relation  $L = \frac{\lambda}{i}$ . The inductance profile (Figure 4.3.1) was found to incur a periodicity of  $60^\circ$  as expected, with one peak corresponding to each of the 6 stator phases. The profile at low and high speeds was found to be almost similar at low and high speeds, with the peaks being slightly higher at low speeds. This difference could possibly because of a quantisation error occurring due to the finite time step used in simulation, because in ideal circumstances the inductance profile is dependent on the construction of the machine and not its speed.

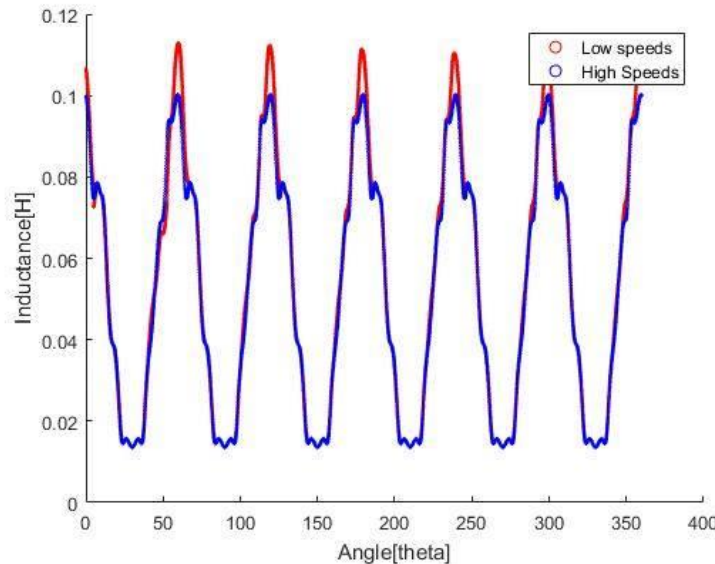


Figure 4.3.1: Calculated inductance profile for of 4 kW, 4-phase, 8/6 pole Oulton, TASC, SRM

From the plot, it can be observed that the maximum inductance value of 110 mH first occurs at  $0^\circ$  and then after every  $60^\circ$ . The minimum inductance value of 15 mH occurs first at  $30^\circ$  and repeats every  $60^\circ$  as well.

### 4.4 Using capacitor for excitation

In the case of the 6/4 machine, generation was carried out using a battery as the energising element (Figure 4.4.1). A battery has a constant voltage across it, which is not the case with actual loads. To make the scenario more realistic, the battery was replaced by a capacitor in the 8/6 machine so that it could have variable voltage. The capacitor was charged to an initial voltage of 150V to provide excitation to the generator.

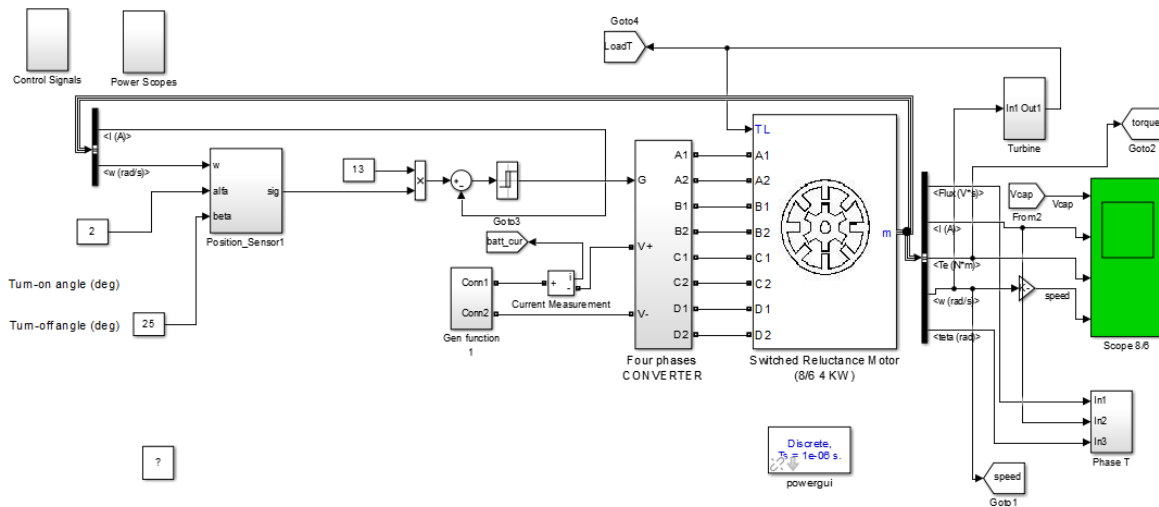


Figure 4.4.1: Simulink model for generation using 8/6 SRM

The simulation was carried out at various values of capacitance. At low values, the sustenance of generated energy was absent due to the limited charge-holding capacity of the capacitor. For higher capacitances, this problem was not encountered. This way, an optimum capacitance was found which could sustain the generated energy. However, another problem cropped up in this case: upon the onset of generation, a large amount of energy was fed back into the capacitor due to which the capacitor voltage was found to shoot up tremendously (Figure 4.4.2). This is because the capacitor was used in isolation, in absence of a resistance through which it could be discharged.

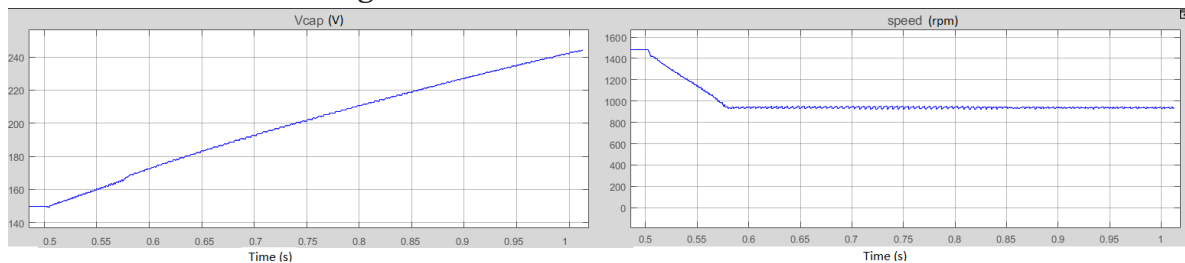


Figure 4.4.2: Infinite charging of capacitor in absence of dissipative element

## 4.5 Using buck converter at load end

To counter the problem faced due to usage of capacitors in isolation, a buck-converter arrangement (Figure 4.5.1) was used at the load end as mentioned in literature [1][8]. The load was taken as an R-L load supplied by a buck converter consisting of a capacitor, an IGBT switch and a freewheeling diode.

The IGBT switch was fed with gate signals obtained using current limit control applied to the load. This allowed the load to be continually supplied, with the load voltage remaining almost constant. (Figure 4.5.2).



## Chapter 5

### MAXIMUM POWER POINT TRACKING USING 8/6 SRG

#### 5.1 Tracking reference rotor speed using turbine characteristics

In order to track the maximum power point (MPP) with changing wind speeds, the wind turbine characteristics were used. The equations governing the wind turbine model in Simulink are given by [14]:

$$C_p(\lambda, \beta) = c_1 \left( \frac{c_2}{\lambda_i} - c_3\beta - c_4 \right) e^{\left( \frac{-c_5}{\lambda_i} \right)} + c_6\lambda \quad (5.1.1)$$

$$\frac{1}{\lambda_i} = \frac{1}{(\lambda + 0.08\beta)} - \frac{0.035}{\beta^3 + 1} \quad (5.1.2)$$

The values of constants are:  $c_1 = 0.5176$ ,  $c_2 = 116$ ,  $c_3 = 0.4$ ,  $c_4 = 5$ ,  $c_5 = 21$  and  $c_6 = 0.0068$ . Here, all quantities are in their p.u. value. For a given wind speed, the maximum power point is obtained when pitch angle  $\beta = \beta_{nom} = 0^\circ$  and  $\lambda = \lambda_{nom} = 8.1$ , that is when the wind strikes perpendicular to the turbine and at an optimum value of  $\lambda$ . For tracking the MPP, we set the generator speed to a reference which was tracked by the PI controller (Appendix A.3). This led to a very fast response allowing the generator to reach the speed which would yield maximum power. The reference speed was given as:

$$\omega_{ref} = v_{wind} * \frac{\lambda_{nom}}{\text{Gear ratio (turbine: generator)}} \quad (5.1.3)$$

#### 5.2 Performance in dynamic wind speed conditions

Initially the wind speed was 9.6 m/s from 0.5s to 2s (Figure 5.2.1). The generator was first allowed to reach its rated speed at 1500 rpm.

After the generation operation was started at 0.5s, it took 0.095s for the generator to reach the speed corresponding to MPP. At 2s, the wind speed was suddenly changed to 12 m/s for which the generator took 0.01s to reach the new MPP. Thus, the generator was able to continuously track MPP.

Table 5.2.1: Power supplied and converted with MPPT

Wind Speed (m/s)	MPP power (p.u.)	MPP (kW)	Turbine Power output (kW)	Machine Power output (kW)	Electrical Power Delivered (kW)
9.6	0.3405	1.2258	1.228	1.186	0.7662
12	0.667	2.401	2.398	2.334	1.857

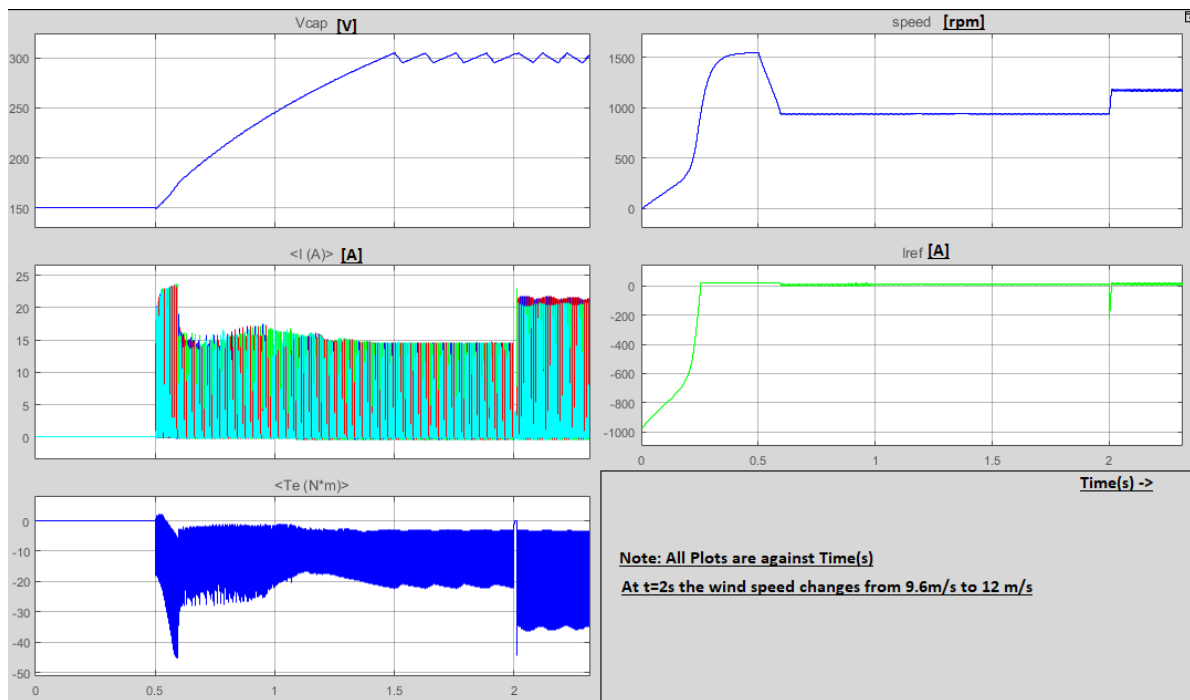


Figure 5.2.1: Simulation result for tracking maximum power point with changing wind speed

At each wind speed, the MPP power (p.u.) was obtained from the turbine characteristics (Figure 5.2.2). Accordingly, the MPP power in kW was calculated. The turbine power obtained at the tracked MPP was found to be very close to this calculated value, thus indicating that the tracking was done correctly. Consequently, the generator was able to convert a significant fraction of the supplied mechanical power. These results have been tabulated in Table 5.2.1.

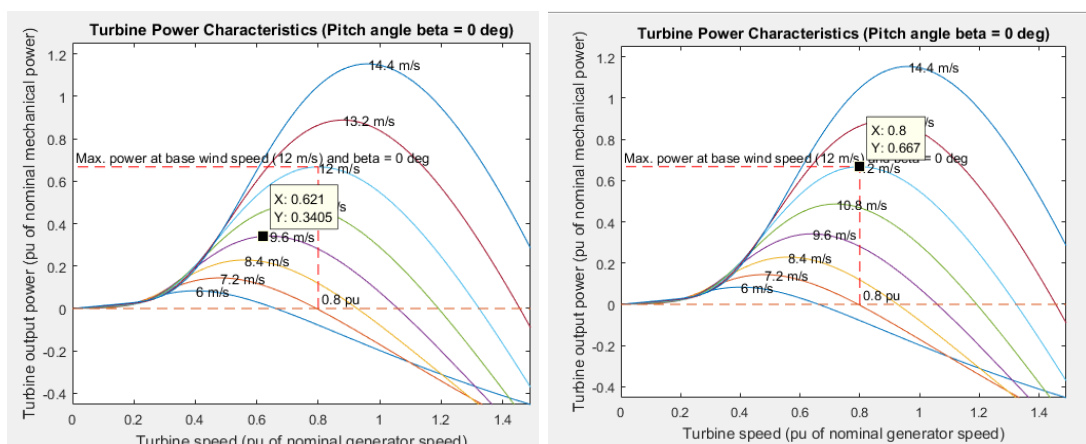


Figure 5.2.2: Turbine characteristic showing maximum power point at 9.6 m/s (left) and 12 m/s (right)



---

## Chapter 6

### CONCLUSION

#### 6.1 Objectives met

- Simulation of SRM in generation mode
- Maximum power point tracking in Wind Energy Conversion System

#### 6.2 Steps involved

- Literature Study of SRM and SRG
- Plot and studied the inductance profile for finding the appropriate  $\theta$  values corresponding to generation.
- Validated the possibility of generation through regenerative braking.
- Simulation of 6/4 SRM in generation mode using battery.
- Procured the magnetisation characteristics of 8/6 Oulton 4 kW SRM drive
- Simulation of 8/6 SRM in generation mode using capacitor and buck converter.
- Introduced a PI controller to track the MPP for variable wind speed

#### 6.3 Conclusion

- Simulated the generation operation of Switched Reluctance Machine with optimum values of  $\theta$  so as to reduce the ripple in the torque and consequently the output Power.
- Employed a buck converter that would maintain constant Voltage at the capacitor end and provide continuous power to the load.
- Successfully tracked the MPP using the PI controller for dynamic wind speed operation by controlling the I reference of hysteresis controller.

---

## APPENDIX A

### A.1 Specifications of the 6/4 Pre-set Machine

Rated power, $P_{\text{rated}}$	:	60 kW
Rated speed, $\omega_{\text{rated}}$	:	3000 rpm
Stator resistance per phase, $R_s$	:	$0.01\Omega$
Inertia, $J$	:	$0.082 \text{ kg-m}^2$
Friction coefficient, $B$	:	$0.01 \text{ N-m-s}$
Minimum inductance, $L_{\text{min}}$	:	$0.67 \text{ mH}$
Maximum inductance, $L_{\text{max}}$	:	$23.6 \text{ mH}$
DC Link Voltage, $V_{\text{DC}}$	:	$240 \text{ V}$
Maximum Current, $I_{\text{max}}$	:	$450 \text{ A}$

### A.2 Specifications of the 8/6 pole Oulton SRM

Rated power, $P_{\text{rated}}$	:	4 kW
Rated speed, $\omega_{\text{rated}}$	:	1500 rpm
Stator resistance per phase, $R_s$	:	$0.747 \Omega$
Inertia, $J$	:	$0.008 \text{ kg-m}^2$
Friction coefficient, $B$	:	$0.005 \text{ N-m-s}$
Minimum inductance, $L_{\text{min}}$	:	$15 \text{ mH}$
Maximum inductance, $L_{\text{max}}$	:	$110 \text{ mH}$
DC Link Voltage, $V_{\text{DC}}$	:	$300 \text{ V}$
Maximum Current, $I_{\text{max}}$	:	$22 \text{ A}$

### A.3 PI controller specifications

Proportional Gain, $K_p$	:	10
Integral Gain, $I$	:	1

## Bibliography

1. T.J.E. Miller " Electronic Control of Switched Reluctance machines" *Newnes Power Engineering Series*, 2001.
2. R. Krishnan, " Switched Reluctance Motor Drives: Modeling, Simulation, Analysis, Design, and Applications" CRC press. 2001.
3. P. Lawrenson, "Switched Reluctance Motor Drives" *IEEE Electronics and Power*, 1983 Pages: 144-147.
4. Nihat Inanc and Veysel Ozbulur, "Torque Ripple Minimization of a switched reluctance motor by using continuous sliding mode control technique" *Electric power Systems Research*, Elsevier, 2003. Pages 241-251.
5. I. Hussain and M.Ehsani, "Torque Ripple Minimization in a Switched Reluctance Motor by PWM Current Control", *IEEE Trans. on PE*, Jan 1998 Pages:83-88.
6. M.Ehsani et.al, "Elimination of Discrete position sensor and current sensor in Switched Reluctance Motor Drives" *IEEE Trans on IA*, Jan-Feb 1992, Pages:128-135.
7. Divya G. and Raman Kalpathi, "Regenerative Braking Using Switched Reluctance Generator" in *International Journal of Scientific & Engineering Research*, Volume 5, Issue 4, April 2014.
8. Roberto Cárdenas et al, "Control of a Switched Reluctance Generator for Variable-Speed Wind Energy Applications," in *IEEE transactions on energy conversion*, vol. 20, no. 4, December 2005. Pages 781-791.
9. Ian Boldea, "Variable Speed Generating Systems" CBS Publishers and Distributors, 2005, pp. 9.1-9.36
10. David Torrey, "Switched Reluctance Generators and their controls", *IEEE Trans on IE*, Feb 2002. Pages 3-14.
11. J.M.D. Murphy and F.G. Turnbull "Power Electronic Control of AC Motors", Pergamon Press, 1988.
12. Don Scansen 'Wind Energy Harvesting' [Online]. Available: <https://www.digikay.in/en/articles/techzone/2012/jul/wind-energy-harvesting> [Accessed: 14-Nov-2017]
13. V.K. Sharma, S. S. Murthy and B. Singh "An Improved Method for the Determination of Saturation Characteristics of Switched Reluctance Motors" in *IEEE trans. Inst. and meas.*, vol. 48, no. 5, October 1999, pp. 995-1000
14. Siegfried Heier, "Grid Integration of Wind Energy Conversion Systems," John Wiley & Sons Ltd, 1998, ISBN 0-471-97143-X

## LIST OF PAPERS BASED ON THESIS

1. S. Roy, M. Jain and G. Bhuvaneswari “Choice of Optimal Dwell Angle in SRG Based Wind Energy Conversion System” *Power & Energy Systems: Towards Sustainable Energy 2018* (submitted)